



Effects of pH and salinity on the separation of magnesium and lithium from brine by nanofiltration

Yan Li^{a,b,c}, Youjing Zhao^{a,b}, Min Wang^{a,b,*}

^aKey Laboratory of Comprehensive and Highly Efficient Utilization of Salt Lake Resources, Qinghai Institute of Salt Lakes, Chinese Academy of Sciences, Xining 810008, China, Tel. +86 971 6313624; emails: marliy001@163.com (M. Wang), gxflwm@126.com (Y. Li), zhaoyj@isl.ac.cn (Y.J. Zhao)

^bKey Laboratory of Salt Lake Resources Chemistry of Qinghai Province, Xining 810008, China

^cUniversity of Chinese Academy of Sciences, Beijing 101408, China

Received 18 May 2017; Accepted 7 November 2017

ABSTRACT

It is difficult to extract lithium because of the high ratio of Mg^{2+} and Li^+ in most salt lake brines in China. Therefore, the separation process of high Mg^{2+}/Li^+ ratio salt lake brine by a negatively charged DK nanofiltration membrane was investigated. The stability of the nanofiltration membrane, the concentration polarization phenomenon, and the surface charge of the nanofiltration membrane was first explored. The ability of the membrane to separate Mg^{2+} and Li^+ at different salinities and pHs was further evaluated. The results indicate that due to the viscosity variation of the solution and the concentration polarization phenomenon, the membrane flux decreases with rising salinity. The Donnan exclusion, dielectric exclusion, and steric hindrance were studied to characterize the ionic fractionations of the nanofiltration membrane. When the salinity was 35 g/L, the Mg^{2+}/Li^+ reduced to 1.49. The membrane flux remained constant at different pHs, and the retention factor of Mg^{2+} was always higher than that of Li^+ . It remained at a relatively high level because of the electrostatic interaction between the cations and the negative charge on the functional groups on the membrane surface. The difference of the cation characters makes the retention factor of Mg^{2+} higher. The separation effect was relatively better under lower pH conditions.

Keywords: Nanofiltration; Separation of Mg^{2+}/Li^+ ; Salinity; pH

1. Introduction

Lithium, the lightest metal element in nature, is mainly obtained from minerals and salt lake brine [1,2]. It is widely used in greases, batteries, refrigerants, and among many other practical applications [3–6]. Lithium resources are rich in most salt lake brine of China. For example, there are roughly 30 saline in the Qaidam Basin, which account for 81% of the total lake saline [7,8]; and the total lithium resources in the lakes are about 3.3 m [9]. Most salt lake brine in China, however, has a high mass ratio of Mg/Li of 40:1 in a majority of salt lake brine, and the highest mass ratio of Mg/Li is

roughly 1,837:1 [10–13]. Moreover, the ionic radius of lithium is similar to that of magnesium. All of these factors limit the development of lithium extraction technology from salt lake brine in China.

The primary methods for lithium extraction from salt lake brine include precipitation [14], extraction [15], adsorption [16], electrolysis [17], and nanofiltration [18]. As an emerging pressure-driven separation technology, nanofiltration stands between ultrafiltration and reverse osmosis [18]. Compared with other technologies of lithium extraction from salt lake brine, the energy consumption of nanofiltration is considerably lower. Additionally, the nanofiltration method

* Corresponding author.

is environmentally friendly, as no additional chemical reagents are needed. Most of the nanofiltration membranes contain charged groups [19–21], which are beneficial for the separation of magnesium and lithium. Because the pore size of the nanofiltration membrane is about 1 nm, corresponding to a molecular weight cut-off of 300–500 Da [22], the nanofiltration process exhibits different retention factor properties for monovalent ions vs. divalent/multivalent ions. Therefore, it can be used for the separation of magnesium and lithium. Many investigations have been conducted on the separation of lithium from salt lake brine by nanofiltration. For example, Somrani et al. [23] compared the separation of lithium from salt lake brines by using nanofiltration and reverse osmosis technology. The results showed that nanofiltration could efficiently separate magnesium and lithium under low flow-rate ratio conditions. Wen et al. [18] studied the process of lithium extraction using a Desal-5 DL membrane. The effects of Donnan exclusion, dielectric exclusion, and steric hindrance on nanofiltration performance were investigated, and the results showed that steric hindrance plays a significant role in the fractionation of various ionic species at high concentration levels of feed. This is because the ionic radius and the mean pore radius of the Desal-5 DL membrane were similar.

The aim of the present work was to study the applicability of nanofiltration in separating lithium from salt lake brine containing a high mass ratio of Mg²⁺ and Li⁺. The separation of Mg²⁺ and Li⁺ at different salinities and pHs was investigated. The variations of the membrane flux, the retention factor of magnesium and lithium, the membrane separation factor, and the mass ratio of Mg²⁺ and Li⁺ in the permeation were analyzed.

2. Theory

2.1. Concentration polarization in the nanofiltration separation process

In pressure-driven membrane separation, the solute and solvent are carried to the membrane surface by convective transport, where the solvent easily passes through the membrane and the retained solute induces increase in local concentration; meanwhile, the rejected solute diffuses back into the bulk solution [24]. When the rate of convective transport of the solute toward the membrane surface is equal to the rate of solute leakage through the membrane plus the rate of the solute because of back-diffusion, the system reaches a steady state and the concentration gradient is formed in the boundary layer; that is, concentration polarization appears in the nanofiltration [24]. The physical model of the mass transport through the boundary layer and through the nanofiltration membrane layer is shown in Fig. 1.

As can be seen in this figure, a material balance in the boundary layer under steady state can be written qualitatively as the following [24,25]:

$$Jc = Jc_p - D \left(\frac{dc}{dy} \right) \quad (1)$$

where “-” indicates the solute diffusing back into the bulk solution in the direction opposite to the solute leakage through the membrane. By integrating Eq. (1) with the

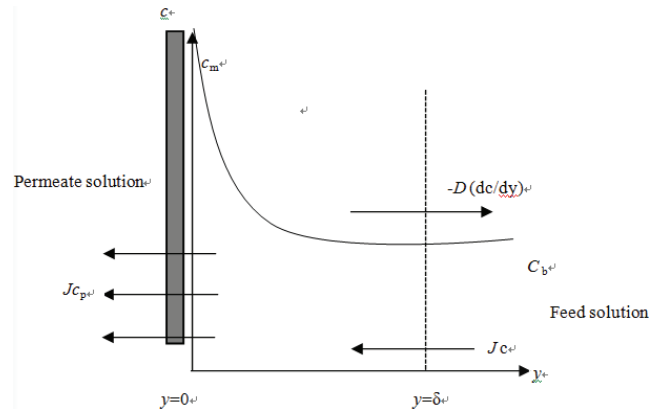


Fig. 1. Concentration polarization at a membrane surface.

boundary conditions: $y = 0, c = c_m$; $y = \delta, c = c_b$, the following equation is obtained:

$$J = \left(\frac{D}{\delta} \right) \ln \frac{c_m - c_p}{c_b - c_p} \quad (2)$$

Here, $k = \frac{D}{\delta}$ is defined as the overall mass transfer coefficient of the solute in the boundary layer, therefore, Eq. (2) can be written as:

$$J = k \ln \frac{c_m - c_p}{c_b - c_p} \quad (3)$$

In membrane separation, the separation performance of the membrane can be represented by the observed retention factor, defined as:

$$R_{\text{obs}} = \left(1 - \frac{c_p}{c_b} \right) \times 100\% \quad (4)$$

However, the solute concentration at the membrane surface is higher than that in the feed due to the effect of concentration polarization. Since the solute rejected by the membrane is the solute concentration at the membrane surface, the intrinsic retention factor is defined as:

$$R_{\text{int}} = \left(1 - \frac{c_p}{c_m} \right) \times 100\% \quad (5)$$

where c_m is difficult to measure directly, but it can be related by Eqs. (2) and (5) by the following expression:

$$\beta = \frac{1}{R_{\text{int}} + (1 - R_{\text{int}}) e^k} \quad (6)$$

where β is the polarization modulus, defined as $\frac{c_m}{c_b}$, and is related to J and k . The overall mass transfer coefficient k can be obtained by the following equation [34]:

$$\text{Sh} = \frac{k d_h}{D} = a \text{Re}^b \text{Sc}^c \left(\frac{d_h}{L} \right)^d \quad (7)$$

where Sc is the Schmidt number, defined as $\frac{\mu}{\rho D}$; a, b, c are constants and vary with the flow regime [26–28]; the Sherwood number may change under different flow conditions [29–31]:

$$\text{For laminar flow: } Sh = 1.62 \left[ReSc \left(\frac{d_h}{L} \right) \right]^{0.33} \quad (8)$$

$$\text{For turbulent flow: } Sh = 0.023 Re^{0.875} Sc^{0.25} \quad (9)$$

It can be seen from Eqs. (8) and (9) that the main factors influencing the overall mass transfer coefficient (k) are $v, D, \rho,$ and $\mu,$ which will influence the concentration polarization in the membrane separation process.

2.2. Calculation in the separation of magnesium and lithium

The permeate was collected in the measuring cylinder, and the permeation flux (J_v) can be calculated as follows:

$$J_v = \frac{V}{A \times t} \quad (10)$$

The observed retention factor (R_{obs}) of Mg^{2+} and Li^+ is calculated by Eq. (4). The separation factor (SF) of the membrane used to express the separation efficiency of the systems can be defined as follows:

$$SF = \frac{\left(\frac{c_{Mg^{2+}}}{c_{Li^+}} \right)_f}{\left(\frac{c_{Mg^{2+}}}{c_{Li^+}} \right)_p} \quad (11)$$

When $SF = 1,$ magnesium and lithium are not separated; when $SF > 1,$ Li^+ penetrates the membrane preferentially and the separation effect becomes better when SF is larger.

3. Materials and methods

3.1. Membrane

Nanofiltration membrane DK-1812 (General Electric Company, USA), a spiral-wound membrane, was used in the experimental runs, which is a composite-type with an active area of $0.38 \text{ m}^2.$ No further information about the membrane charge properties was provided by the manufacturer.

3.2. Standards and reagents

Magnesium chloride hexahydrate ($MgCl_2 \cdot 6H_2O,$ AR, Sinopharm Chemical Reagent Co., Ltd., Shanghai, China) and lithium chloride ($LiCl,$ AR, Shanghai Macklin Biochemical Co., Ltd., Shanghai, China) were used to prepare the simulated brine and the mass ratio of Mg^{2+} and Li^+ was 35. All salts were dissolved in deionized water with a resistivity more than $18 \text{ M}\Omega \text{ cm}$ obtained by a reverse osmosis membrane (UPT-11-20T, China). All solutions were preprocessed by filter device to remove the impurity which could pollute the

nanofiltration membrane. Table 1 shows the hydrated radius and the diffusion coefficient of the solutes [32–34].

3.3. Membrane test unit

Fig. 2 depicts the membrane test unit characterizing of the nanofiltration separation device. A laboratory-scale nanofiltration test unit (DSP-1812W-S, Hangzhou Donan Memtec Co., Ltd., China) was used for the membrane study. The feed was pumped to the membrane module after removing the impurities by filtering through a filter. The flow rates of the concentrated solution were measured using a flow meter; the temperature of the feed solution was controlled by circulating with cool/hot water; and the pressure was controlled by a pressure regulating valve. After each experiment, the system was cleaned three times by circulating demineralized water at a temperature of $25^\circ\text{C} \pm 0.5^\circ\text{C}$ for 5 min and at a pressure of $3.5 \pm 0.01 \text{ MPa}.$ The membrane should be kept in a sealed container with 0.5% sodium bisulfite if the system shuts down for a long time. The temperature of the feed solution was maintained constant by circulating cool/hot water, and the transmembrane pressure was maintained at $3.5 \pm 0.01 \text{ MPa}.$ Samples of permeate and feed were collected after recirculation of both solutions until the system reached the steady state. It is necessary to clean the membrane using chemical and physical methods when the membrane flux or the retention factor dropped significantly.

Table 1
The hydrated radius and the diffusion coefficient of the solutes

	Mg^{2+}	Li^+	H^+	Cl^-
Hydrated radius (nm)	0.428	0.382	0.280	0.332
Diffusion coefficient $D/(10^4 \text{ m}^2/\text{S})$	0.720	1.030	9.310	2.030

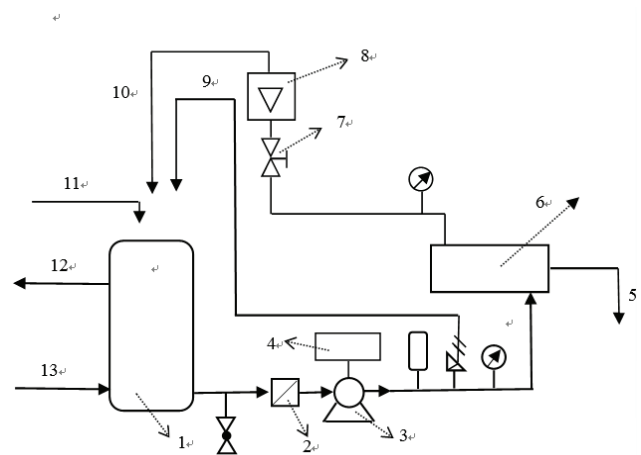


Fig. 2. Experimental setup of the nanofiltration separation device. 1, Feed tank; 2, pipe filter; 3, pump; 4, inverter; 5, permeate; 6, nanofiltration module; 7, pressure regulating valve; 8, concentrate flow meter; 9, overflow liquid; 10, concentrate pipe; 11, feed; and 12 and 13, cool/hot water.

3.4. Experimental procedure

3.4.1. Determination of zeta potential

The streaming potential of the membrane was measured using a streaming potential analyzer (SurPass 3, Anton Paar Trading Co., Ltd., Austria). This apparatus was described in detail in Elimelech et al. [35] and Childress and Elimelech [36]. The membrane was cut into 10 × 20 mm pieces to fit the rectangular cell after rinsing and soaking in deionized water for 24 h. Two pieces of membrane attached to the cell were used for each measurement, which were positioned opposite to one another with their active layer side and separated with spacers to create a channel flowing through the solutions. The mixed salt test solutions (MgCl₂ and LiCl) were used for evaluating the streaming potential of the membrane at different salinities (15–65 g/L) and pHs (3–9). The pH was adjusted from the initial value of about 6.5–9 by addition of NaOH. HCl was then added to lower the pH to a final value of 3.

3.4.2. The pure water permeability of the membrane

The nanofiltration membrane was conditioned at different operating pressures 0.5–3.5 MPa to study the pure water permeability using deionized water and the temperature was controlled steadily at 25°C ± 0.5°C. The concentrate flux of 120.0 L/h was used in the pure water permeability experiment. The membrane system was allowed to equilibrate for 5 min.

Kedem and Katchalsky [37] proposed that the relationship between the driving force and the flux can be expressed by the flux of the pure water:

$$J_V = L_p(\Delta P - \sigma\Delta\Pi) \quad (12)$$

where L_p is only related to the temperature and the membrane structure parameters. If pure water is on both sides of the nanofiltration membrane, $\Delta\Pi$ is zero without osmotic pressure. Then, the pure water flux can be defined as follows:

$$J_V = L_p\Delta P \quad (13)$$

The pure water permeability L_p was obtained based on the relationship between the pure water flux and the pressure. The membrane needs to be replaced if L_p fluctuates greatly.

3.4.3. Membrane separation of lithium and magnesium at different salinities and pHs

The nanofiltration membrane test unit was conditioned at a constant operating pressure (3.5 ± 0.01 MPa) using solutions of different salinities (15–65 g/L) and different pH values (over the pH range of 3–5) with MgCl₂ and LiCl. The concentrate flux of 120.0 L/h was used. The concentration and permeate solutions were obtained after the membrane system equilibrated for 5 min. The membrane test unit was flushed thoroughly with deionized water three times and rinsed with a salt solution for each experimental run using a new salt solution each time. The temperature of test solution was maintained at 30°C ± 0.5°C. Three experiments were done for each experimental condition and the error bars are based on the experimental results.

3.5. Analytical methods

Inductively coupled plasma (ICP; ICAP6500 Spectrometer, USA) was used to investigate the Li⁺ concentration. Meanwhile, the concentration of Mg²⁺ was determined by titration with 0.04539 M Ethylene Diamine Tetraacetic Acid and the analytical error is ±0.2%. The temperature of the feed was measured using an infrared thermometer. The pH of the feed was adjusted by 1 M HCl, and the pH values of the solutions were measured using a pH meter (S210, Mettler-Toledo Instruments Co., Ltd., Shanghai). The viscosity of the solutions was measured using a rotating viscometer (NDJ-8S, Nirun Intelligent Technology Co., Ltd., Shanghai).

4. Results and discussion

4.1. Membrane zeta potential

The zeta potential of the DK nanofiltration membrane as a function of salinity (15–65 g/L) at constant pH (pH = 5.5) for salt solutions (MgCl₂ and LiCl) is given in Fig. 3 and the zeta potential of the DK nanofiltration membrane as a function of pH (over the pH range 3–6) at constant salinity (25 g/L) for salt solutions (MgCl₂ and LiCl) is given in Fig. 4. The figures reveal the following: (1) the membrane is negatively charged over the entire pH/salinity range investigated; (2) the zeta potential becomes more negative as the pH/salinity increases. It is suggested that the adsorption of anions (Cl⁻ and OH⁻) from the solution controls the membrane surface charge status [35]. Because anions in solutions are less hydrated than cations [35], anions can miss the bound moisture and approach the membrane surfaces more favorably. The concentration of Cl⁻ and OH⁻ in the solution increases with increased salinity (MgCl₂ and LiCl) and pH, respectively. More anions can be absorbed by the nanofiltration membrane and the membrane zeta potential becomes more negative.

4.2. The pure water permeability of the membrane

Fig. 5 illustrates the variation of the pure water flux vs. the applied pressure. The results exhibit that the pure water

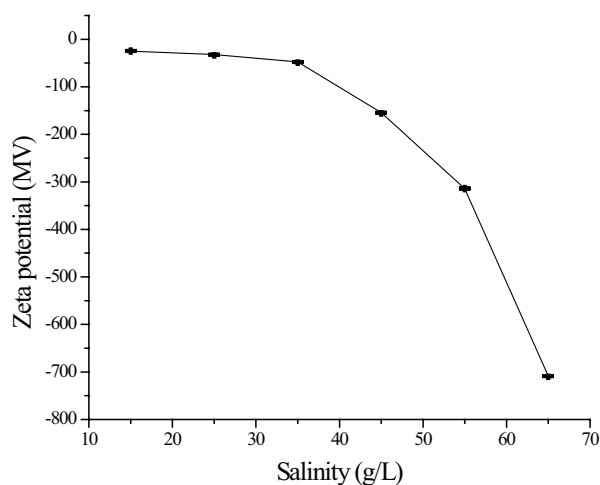


Fig. 3. Zeta potential of the DK nanofiltration membrane as a function of salinity for the DK-1812 membrane and MgCl₂ and LiCl brine system at a constant pH (pH = 5.5) condition.

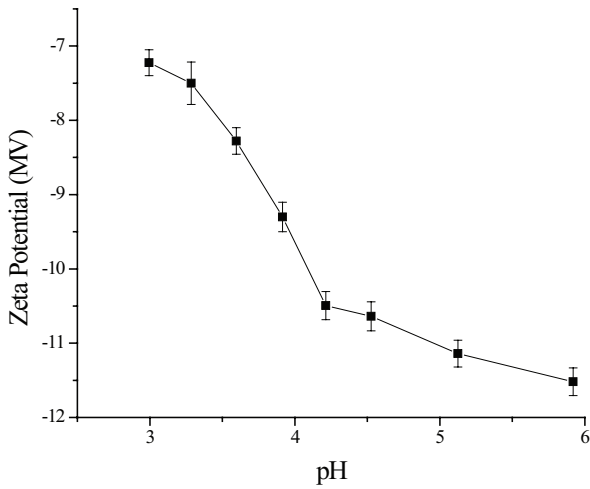


Fig. 4. Zeta potential of the DK nanofiltration membrane as a function of pH for the DK-1812 membrane and MgCl₂ and LiCl brine system at a constant salinity (25 g/L) condition.

flux of the DK nanofiltration membrane increases linearly with the applied pressure and the pure water permeability $L_p = 1.312 \times 10^{-11}$ m/(s Pa), which shows that the nanofiltration membrane has a good stability within 0.5–3.5 MPa. The pure water permeability in this study for the DK nanofiltration membrane is in line with the one reported by Straatsma et al. [38], but is lower than those reported by Hagemeyer and Gimbel [39], Bargeman et al. [40], and Bowen and Mohammad [41] (Table 2). The possible explanations for the differences in pure water permeability include different measurement methods, different module configuration, and different representativeness of the small membrane sheets used [40].

4.3. Membrane separation of lithium and magnesium at different salinities

4.3.1. Effect of salinity on membrane flux

The relationship between the DK membrane flux and salinity is listed in Fig. 6. As can be seen from Fig. 6, the membrane flux decreases significantly with increasing salinity. It can be seen from Eqs. (8) and (9) that the overall mass transfer coefficient (k), which is related to the polarization modulus, is influenced by v , D , ρ , and μ . The diffusion coefficient, D , of the solutes is influenced by the viscosity. They can be related as follows [42,43]:

$$D = D_o \times \frac{T}{T_o} \times \frac{\mu_o}{\mu} \tag{14}$$

It was reported that the viscosity of the solution was affected by the salt concentration, where the solution viscosity increases with increasing salt concentration [25] which can be proved in Table 3. With the increase of salt concentration, more Cl⁻ in the solution is adsorbed in the membrane. A great number of Cl⁻ accumulates to form an electric double layer in/on the nanofiltration membrane pores, increasing the electroviscous effect [44]. This reduces both the diffusion coefficient and the membrane flux. The concentration polarization also decreases the membrane flux, which is due to the

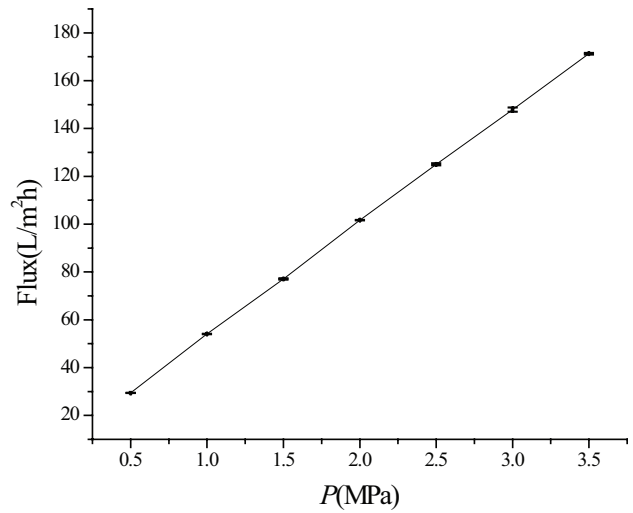


Fig. 5. Pure water flux as a function of the applied pressure. Operating conditions: the temperature, 30°C ± 0.5°C and the concentrate flux, 120.0 L/h.

Table 2
Pure water permeability reported for different DK nanofiltration membranes

Membrane	Pure water permeability 10 ⁻¹¹ m/(S Pa)	Reference
Desal-5 DK	1.5	Bargeman et al. [40]
Desal-5 DK	1.3	Straatsma et al. [38]
Desal-5 DK	1.4	Bowen and Mohammad [41]
Desal-5 DK (the first batch)	2.2	Hagemeyer and Gimbel [39]
Desal-5 DK (the second batch)	1.7	Hagemeyer and Gimbel [39]
DK-1812	1.3	This study

increase in osmotic pressure, $\Delta\Pi$, with the increase in salinity. According to Jiratananon et al. [45], the osmotic pressure is mainly responsible for the flux decline. Eq. (12) also indicates that increase of osmotic pressure reduces the driving force ($\Delta P - \sigma\Delta\Pi$), resulting in a lower membrane flux.

4.3.2. Effect of salinity on the separation of lithium and magnesium

The mass transport through the nanofiltration membrane is affected by a combination of the Donnan exclusion, dielectric exclusion, and steric hindrance [46]. The Donnan exclusion is caused by the electrostatic interaction between the ions in the solution and the fixed charge of the membrane [47]. The higher the co-ion (ion has the same charge with the membrane) charge in the solution, the stronger the repulsion and the higher the counterion (ion has the opposite charge with the membrane) charge; and therefore, the stronger the attraction. Because the membrane is negatively charged, the Donnan exclusion is not conducive for separating Mg²⁺

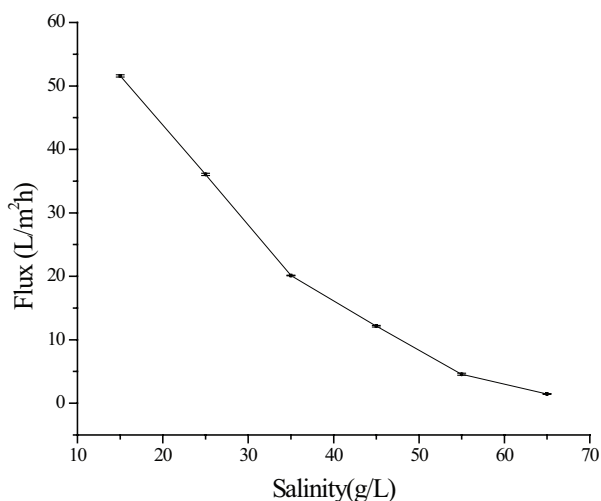


Fig. 6. The DK membrane flux as a function of salinity for the DK-1812 membrane and MgCl_2 and LiCl brine system. Operating conditions: the salinity, 15–65 g/L; the operating pressure, 3.5 MPa; the operating temperature, $30^\circ\text{C} \pm 0.5^\circ\text{C}$; and the concentrate flux, 120.0 L/h.

Table 3

The variation of the viscosity for the solution under different salinity conditions

Salinity (g/L)	Viscosity (mPa s)
15	1.17
25	1.19
35	1.35
45	1.43
55	1.57
65	1.65

and Li^+ . Dielectric exclusion occurs due to the interaction of the ions with the bound electric charges induced by ions at the interfaces between media of different dielectric constants [48]. The dielectric exclusion is proportional to the square of the ionic valence, which helps the separation of magnesium and lithium and aids in enhancing the rejection rate of Mg^{2+} . Steric hindrance plays a role in separating the solute ions dependent on ionic radii, particularly when the ionic radii are correlated with the pore radius of the nanofiltration membrane [18].

The separation (observed retention factor) of MgCl_2 and LiCl salt solutions by the nanofiltration membrane as a function of salinity is given in Fig. 7. Based on Fig. 7, the following results are made: (1) The retention factor of Mg^{2+} increased first and then decreased with salinity in the range of 15–65 g/L and reached maximum of 93% at 35 g/L (Fig. 7). The retention factor of Mg^{2+} is always higher than that of Li^+ , which may be due to the following: Donnan exclusion has a more remarkable effect on Mg^{2+} to pass through the membrane than on Li^+ , but as shown in Table 1, the hydrated radius of Li^+ is smaller than that of Mg^{2+} and the diffusion coefficient of Li^+ is larger than Mg^{2+} . In this manner, Li^+ can pass through the membrane more easily. Conversely, the dielectric exclusion is proportional to the square of the ionic valence, which benefits Li^+

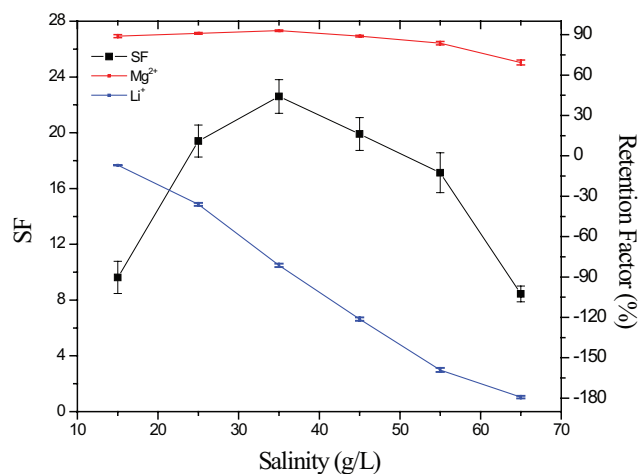


Fig. 7. Effect of salinity on retention factor of Mg^{2+} and Li^+ and on SF. Operating conditions: the salinity, 15–65 g/L; the operating pressure, 3.5 MPa; the operating temperature, $30^\circ\text{C} \pm 0.5^\circ\text{C}$; and the concentrate flux, 120.0 L/h.

but is detrimental to Mg^{2+} to pass through the nanofiltration membrane. Furthermore, with higher concentrations of feed, steric hindrance might be enhanced. Table 1 shows the ionic radii of the ions in consideration. It can be seen that the ionic radii are comparable with the mean pore radius of the DK membrane (0.42 nm [40]). Thus, the DK can exhibit good steric partitioning of ions, with the potential for rejection following this sequence: $\text{Mg}^{2+} > \text{Li}^+$. When the salinity was in the range of 45–65 g/L, the decreasing retention factor of Mg^{2+} can be explained as follows [49]:

$$J_s = P_s(\beta c_f - c_p) \quad (15)$$

From Eq. (15), the flux of solute J_s is a function of the concentration on both sides of the membrane. And the osmotic pressure $\Delta\Pi$ increases with increasing salinity, which can reduce the water flux. The Mg^{2+} concentration in the permeate increases with the decrease of water flux. When the salinity increases constantly, more ions are transported from the bulk solution toward the membrane surface. As shown in Eq. (6) the polarization modulus β increases, which indicates the concentration polarization is enhanced. This can increase the Mg^{2+} flux and decrease the Mg^{2+} retention factor. (2) The retention factor of Li^+ is reduced persistently. This can be explained by the following: the membrane becomes more negative with an increase in salinity (Fig. 3), so the electrostatic interaction between the cations in the solution and the fixed charge of the membrane (Donnan exclusion) is enhanced. More Li^+ with less of hydrated radius and greater diffusion coefficient can go through the membrane, thereby increasing the Li^+ concentration in the permeation. Moreover, the enhanced concentration polarization with increasing salinity can also decrease the retention factor of Li^+ . Additionally, the concentration of Cl^- increases with an increase in the salinity. A potential difference is formed at the separation interface because a large amount of Cl^- can pass through the membrane. Therefore, to maintain electroneutrality, Li^+ passes through the membrane first under the negative concentration gradient. At the same time, the retention factor of Li^+ remains negative because of

the anti-concentration gradient transport and the competitive transmission between the co-ions (Mg^{2+} and Li^+).

Dielectric exclusion decreases as Donnan exclusion increases with the increase of the feed concentration; the dielectric exclusion phenomenon therefore increases the screening of the membrane fixed charge and thus reduces the electric exclusion [46]. The decrease of the dielectric exclusion could reduce the retention factor of Mg^{2+} and prevent the separation of Mg^{2+} and Li^+ [50], which can be proved by the variation of the SF (Fig. 7). The retention factor of Mg^{2+} is always higher than that of Li^+ and the concentration of Li^+ in the permeate increases as the salinity increases, so the SF of the membrane increases first. Then, the SF decreases when the salinity is at 45 g/L, which may be affected by the decrease in the dielectric exclusion. As can be seen from the data variations (Table 4) of the $\text{Mg}^{2+}/\text{Li}^+$ in the permeation, when the salinity is 45 g/L, the concentration of Mg^{2+} in the permeate increased 76.74% compared with that at 35 g/L salinity and even more with continually increasing salinity, and at the same time the $\text{Mg}^{2+}/\text{Li}^+$ in the permeate also increased. It is inferred that when the feed concentration is 45 g/L, the dielectric exclusion experiences a descending trend. As can be seen in Table 4, the yield of Li^+ decreases with increasing salinity though the retention factor of Li^+ is reduced persistently and the concentration of lithium in the permeate increases. This may be explained by the decreasing membrane flux with increasing salinity (Fig. 6). Therefore, the suitable salinity is 25 g/L.

4.4. Membrane separation of lithium and magnesium at different pH

4.4.1. Effect of pH on the membrane flux

The relationship between the DK membrane flux and pH is shown in Fig. 8. As can be seen, the nanofiltration membrane flux decreases slightly and then maintains stable. The flux remains constant within the studied pH, which is consistent with the result of Richards et al. [51] and Mänttari et al. [52] for nanofiltration membranes examined under different pHs. However, for these studies, it could not be concluded that pH did not affect the membrane permeability. For example, the results of Childress and Elimelech [34] for the flux of NF-55 nanofiltration membrane at different pHs revealed that the flux is steady at pH 3–9, but there was a slight peak at pH = 5, which may be due to: (1) the pore size of NF-55 nanofiltration membrane increased because of conformational changes of the cross-linked membrane polymer structure; (2) the electroviscous effect of the solution was decreased; and

(3) the decrease of the osmotic pressure at the membrane surface increased the net driving pressure.

4.4.2. Effect of pH on the separation of magnesium and lithium

Most of the nanofiltration membranes are charged and the property of charges has a great influence on its separation performance. The pH of the feed and the permeate is listed in Table 5. As can be seen from this table, the pH of the permeate is significantly lower than that of the feed. The reason for this might be the following [53,54]: the nanofiltration membrane is negatively charged under the studied pH, so cations can pass through the nanofiltration membrane under the combined force of the Donnan exclusion and electrostatic attraction of the charge on the nanofiltration membrane surface. As can be seen from Table 1, the hydrated radius of H^+ , Mg^{2+} , and Li^+ is: $\text{Mg}^{2+} > \text{Li}^+ > \text{H}^+$ and diffusion coefficient of H^+ , Mg^{2+} , and Li^+ is: $\text{H}^+ > \text{Li}^+ > \text{Mg}^{2+}$. It can therefore be inferred that the sequences of these three ions passing through the nanofiltration membrane are as follows: $\text{H}^+ > \text{Li}^+ > \text{Mg}^{2+}$. Due to the acidic condition of the solutions, a large number of H^+ can pass through the nanofiltration membrane, leading to a lower pH in the permeate than in the feed.

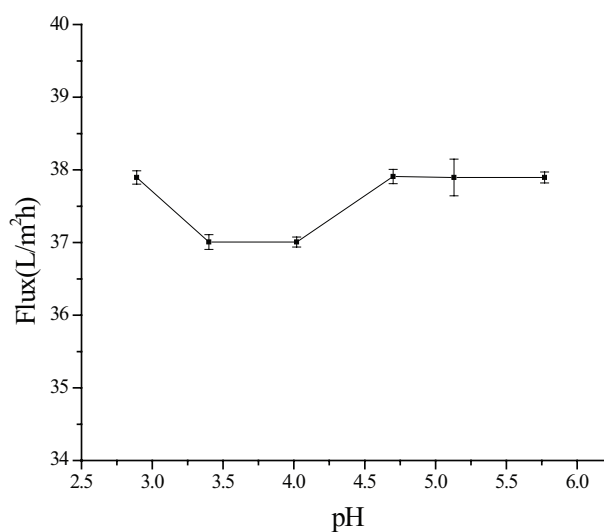


Fig. 8. The DK membrane flux as a function of pH for the DK-1812 membrane and MgCl_2 and LiCl brine system. Operating conditions: pH, 3–5.5; the operating pressure, 3.5 MPa; the operating temperature, $30^\circ\text{C} \pm 0.5^\circ\text{C}$; and the concentrate flux, 120.0 L/h.

Table 4

The variations of the concentration of Mg^{2+} and Li^+ in the permeate and the yield of Li^+ under different salinity conditions

Salinity (g/L)	$c_{p(\text{Mg}^{2+})}$ (g/L)	$c_{p(\text{Li}^+)}$ (g/L)	$\text{Mg}^{2+}/\text{Li}^+$ in the permeate	The yield of Li^+ (%)
15	0.419	0.112	3.729	15.013
25	0.419	0.238	1.763	13.943
35	0.662	0.445	1.489	10.749
45	1.170	0.670	1.746	8.195
55	2.018	0.960	2.103	3.977
65	4.087	1.050	3.892	1.197

Table 5
The pH of the feed and the permeate for the DK-1812 membrane and MgCl_2 and LiCl simulated brine system

Feed pH	Permeate pH
2.89	2.48
3.40	2.97
4.02	3.65
4.70	4.35
5.13	5.04
5.77	5.04

The relationship between the retention factors of Mg^{2+} and Li^+ and pH is examined and shown in Fig. 9, as can be seen, with an increase in pH, the retention factor of Mg^{2+} is always higher than that of Li^+ and remains at a relatively high level. When $\text{pH} < 4$, the retention factor of Mg^{2+} decreases slightly while the retention factor of Li^+ reduces more significantly. This may be due to the following: when $\text{pH} < 4$, the concentration of H^+ in the solution increases with decreasing pH. Because the solution pH can be regulated by adding HCl, the lower the pH, the higher the H^+ concentration. Therefore, the competition between co-ions (Mg^{2+} , Li^+ , and H^+) is more intense, especially for H^+ and Li^+ . As can be seen from Table 1, the hydrated radius of H^+ is less than that of Li^+ and Mg^{2+} , but the diffusion coefficient of H^+ is much greater than that of Li^+ and Mg^{2+} . Thus, a large amount of H^+ in the solution can pass through the nanofiltration membrane first by the electrostatic attraction between the cations and the negative surface charge of the nanofiltration membrane, and the retention factors of Mg^{2+} and Li^+ increase with decreasing pH, especially for Li^+ . As shown in Table 5, the pH of the permeation is lower than that of the feed, suggesting that a large amount of H^+ enters the permeation. When $\text{pH} > 4$, the retention factors for Mg^{2+} and Li^+ remain stable, which may be due to the following: the concentration of H^+ in the solution decreases as the pH increases, but the solution remains acidic. H^+ can still pass through the nanofiltration membrane first and maintain a relatively stable retention factor of Mg^{2+} and Li^+ . The changing trend of retention factor with pH is consistent with the zeta potential changes with pH over the study range of 3–5.5 (Fig. 4), which declines rapidly when $\text{pH} < 4$, but reduces slowly in pH over the range of 4–6.

The relationship between SF of the membrane and pH is listed in Fig. 10. As shown, when $\text{pH} < 4$, the SF of the membrane decreases sharply with pH, which is related to the variation of $\text{Mg}^{2+}/\text{Li}^+$ in the permeate (Fig. 10). The retention factors of Mg^{2+} and Li^+ decreases, and as can be seen from Table 6, the increasing trend of Mg^{2+} concentration in the permeate with pH is clearer than that of Li^+ . Thus, the $\text{Mg}^{2+}/\text{Li}^+$ in the permeate increases, resulting in a decrease in the SF. When $\text{pH} > 4$, with the increases of pH, the SF increases slightly and then decreases slowly, which is in agreement with the variation of $\text{Mg}^{2+}/\text{Li}^+$ in the permeate. The change of the SF can also be due to the initial concentration difference (Table 6) between Mg^{2+} and Li^+ , resulting from the operating error in the preparation of the feed with different pHs. And as can be seen in Table 6, the feed pH has little effect on the yield Li^+ .

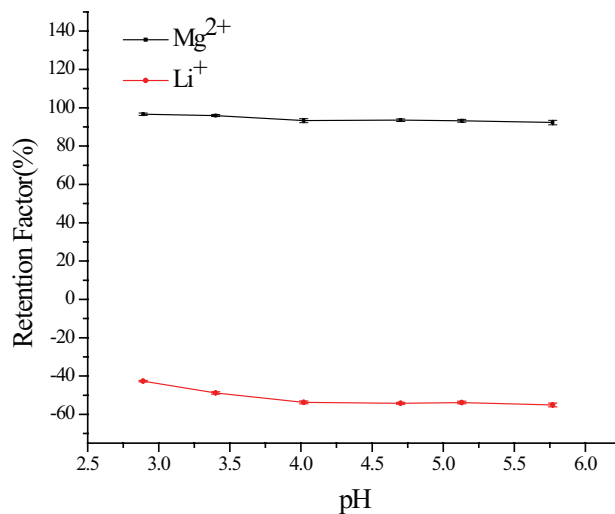


Fig. 9. Effect of pH on retention factors of Mg^{2+} and Li^+ for the DK-1812 membrane and MgCl_2 and LiCl brine system. Operating conditions: pH, 3–5.5; the operating pressure, 3.5 MPa; the operating temperature, $30^\circ\text{C} \pm 0.5^\circ\text{C}$; and the concentrate flux, 120.0 L/h.

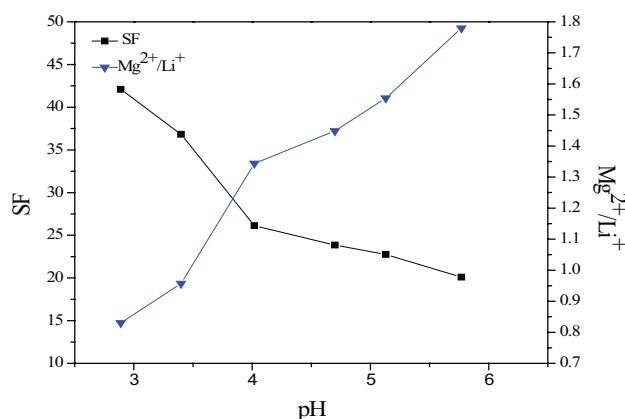


Fig. 10. Effect of pH on SF of the membranes and the mass ratio of Mg^{2+} and Li^+ in the permeation for the DK-1812 membrane and MgCl_2 and LiCl brine system. Operating conditions: pH, 3–5.5; the operating pressure, 3.5 MPa; the operating temperature, $30^\circ\text{C} \pm 0.5^\circ\text{C}$; and the concentrate flux, 120.0 L/h.

5. Conclusion

A DK membrane was used to investigate the possibility of separating Mg^{2+} and Li^+ from a simulated brine with a high $\text{Mg}^{2+}/\text{Li}^+$ ratio. The stability and the surface charge of the DK nanofiltration membrane were investigated, and the results show that the DK nanofiltration membrane exhibits good stability within 0.5–3.5 MPa. The nanofiltration membrane is negatively charged and the zeta potential becomes more negative as the salinity and pH increase. The separation of Mg^{2+} and Li^+ by the nanofiltration membrane at different salinities and pHs was also studied. Results show that the DK nanofiltration membrane flux decreases with increasing salinity and the membrane exhibits a high retention factor for Mg^{2+} , but a poor retention factor of Li^+ by the combination of Donnan exclusion, dielectric exclusion, and steric hindrance.

Table 6

The concentration variation of Mg²⁺ and Li⁺ in the feed and the permeate with different pH and the yield of Li⁺

Feed pH	$c_{f(\text{Li}^+)} \text{ (g/L)}$	$c_{f(\text{Mg}^{2+})} \text{ (g/L)}$	$c_{p(\text{Li}^+)} \text{ (g/L)}$	$c_{p(\text{Mg}^{2+})} \text{ (g/L)}$	The yield of Li ⁺ (%)
2.89	0.186	6.510	0.266	0.221	10.572
3.40	0.186	6.554	0.277	0.265	10.784
4.02	0.187	6.554	0.287	0.386	11.143
4.70	0.188	6.488	0.290	0.419	11.420
5.13	0.185	6.532	0.284	0.441	11.395
5.77	0.184	6.576	0.285	0.506	11.497

When the feed concentration is 35 g/L, the Mg²⁺/Li⁺ in the permeate reduces to 1.49 and the SF is 22.60, the separation performance of magnesium and lithium works best. However, the yield of lithium is 10.8%, which is relatively lower compared with 25 g/L. Additionally, the membrane flux remains constant with pH. The retention factor of Li⁺ decreases from -42.7% at pH 2.89 to -53.7% at pH 4.02 and the retention factor of Mg²⁺ is always higher than Li⁺ and remains at a relatively higher level, which may be due to the fact that H⁺ has a smaller hydrated radius and a greater diffusion coefficient than Mg²⁺ and Li⁺, and therefore, it can pass through the nanofiltration membrane more easily. When the feed pH = 2.89, the Mg²⁺/Li⁺ in the permeation is 0.83 and the SF is 42.09. These results show that the separation performance of magnesium and lithium works better at lower pH conditions.

Acknowledgments

This work was supported by National Natural Science Foundation of China (No. U1507202 and No. 21601197) and Natural Science Foundation for the Youth of Qinghai Province, China (2015-ZJ-934Q).

Symbols

D	—	Diffusion coefficient of the solute, 10 ⁴ m ² /S
c	—	Solute concentrations in the boundary layer, g/L
c_p	—	Solute concentrations in the permeate, g/L
δ	—	Boundary layer thickness, m
c_m	—	Concentration at the membrane surface, g/L
Sh	—	Sherwood number
d_h	—	Hydraulic diameter, m
L	—	Length of the membrane module, m
V	—	Volume of the permeate penetrated through the membrane, L
A	—	Membrane active area, m ²
t	—	Time taken to obtain the permeate, s
SF	—	Separation factor of the membrane
$\left(\frac{c_{\text{Mg}^{2+}}}{c_{\text{Li}^+}}\right)_f$	—	Concentration ratio of the Mg ²⁺ and Li ⁺ in the feed
$\left(\frac{c_{\text{Mg}^{2+}}}{c_{\text{Li}^+}}\right)_p$	—	Concentration ratio of the Mg ²⁺ and Li ⁺ in the permeate
ΔP	—	Applied pressure, MPa
L_p	—	Pure water permeability, m/(S Pa)
$\Delta \Pi$	—	Osmotic pressure, MPa

T	—	Temperature, K
μ	—	Solution viscosity, Pa s
J_s	—	Salt flux, L/m ² s
P_s	—	Salt permeation coefficient
c_f	—	Solute concentrations on the feed, g/L

References

- [1] W. Xiang, S. Liang, Z. Zhou, W. Qin, W. Fei, Extraction of lithium from salt lake brine containing borate anion and high concentration of magnesium, *Hydrometallurgy*, 166 (2016) 9–15.
- [2] F.G. Will, Impact of lithium abundance and cost on electric vehicle battery applications, *J. Power Sources*, 63 (1996) 23–26.
- [3] M.A. Delgado, C. Valencia, M.C. Sánchez, J.M. Franco, C. Gallegos, Thermorheological behaviour of a lithium lubricating grease, *Tribol. Lett.*, 23 (2006) 47–54.
- [4] A. Ritchie, W. Howard, Recent developments and likely advances in lithium-ion batteries, *J. Power Sources*, 162 (2006) 809–812.
- [5] T. Muroga, Vanadium alloys for fusion blanket applications, *Mater. Trans.*, 46 (2005) 405–411.
- [6] U. Schafer, Past and present conceptions concerning the use of lithium in medicine, *J. Trace Microprobe Tech.*, 16 (1998) 535–556.
- [7] S.E. Kesler, P.W. Gruber, P.A. Medina, G.A. Keoleian, M.P. Everson, T.J. Wallington, Global lithium resources: relative importance of pegmatite, brine and other deposits, *Ore Geol. Rev.*, 48 (2012) 55–69.
- [8] S. Yu, The hydrochemical features of salt lakes in Qaidam Basin, *Chin. J. Oceanol. Limnol.*, 4 (1986) 383–403.
- [9] Research in China, China Lithium Carbonate Industry Report, 2009. Available at: <http://www.researchinchina.com/FreeReport/PdfFile/633985558995235000.pdf/>
- [10] X. Liu, X. Chen, L. He, Z. Zhao, Study on extraction of lithium from salt lake brine by membrane electrolysis, *Desalination*, 376 (2015) 35–40.
- [11] K.T. Tran, T.V. Luong, J.W. An, D.J. Kang, M.J. Kim, T. Tran, Recovery of magnesium from Uyuni solar brine as high purity magnesium oxalate, *Hydrometallurgy*, 138 (2013) 93–99.
- [12] F.U. Ye, H. Zhong, Research situation of separating magnesium and lithium from high Mg/Li Ratio Salt Lake brine, multipurpose utilization of mineral resources, *Multipurpose Util. Miner. Resour.*, 2 (2010) 30–32.
- [13] J. Wang, The present status of lithium extraction from Li-bearing brines, *Ind. Miner. Process.*, 12 (1999) 1–5.
- [14] J.W. An, D.J. Kang, K.T. Tran, M.J. Kim, T. Lim, T. Tran, Recovery of lithium from Uyuni solar brine, *Hydrometallurgy*, 117–118 (2012) 64–70.
- [15] Z. Zhou, Q. Wei, S. Liang, Y. Tan, W. Fei, Recovery of lithium using tributyl phosphate in methyl isobutyl ketone and FeCl₃, *Ind. Eng. Chem. Res.*, 51 (2012) 12926–12932.
- [16] C. Özgür, Preparation and characterization of LiMn₂O₄ ion-sieve with high Li⁺, adsorption rate by ultrasonic spray pyrolysis, *Solid State Ionics*, 181 (2010) 1425–1428.
- [17] T. Hoshino, Preliminary studies of lithium recovery technology from seawater by electro dialysis using ionic liquid membrane, *Desalination*, 317 (2013) 11–16.

- [18] X. Wen, P. Ma, C. Zhu, Q. He, X. Deng, Preliminary study on recovering lithium chloride from lithium-containing waters by nanofiltration, *Sep. Purif. Technol.*, 49 (2006) 230–236.
- [19] P. Fievet, C. Labbez, A. Szymczyk, A. Vidonne, A. Foissy, J. Pagetti, Electrolyte transport through amphoteric nanofiltration membranes, *Chem. Eng. Sci.*, 57 (2002) 2921–2931.
- [20] X.L. Wang, T. Tsuru, S.I. Nakao, S. Kimura, Electrolyte transport through nanofiltration membranes by the space-charge model and the comparison with Teorell-Meyer-Sievers model, *J. Membr. Sci.*, 103 (1995) 117–133.
- [21] X.L. Wang, W.J. Shang, D.X. Wang, L. Wu, C.H. Tu, Characterization and applications of nanofiltration membranes: state of the art, *Desalination*, 236 (2009) 316–326.
- [22] A.W. Mohammad, Y.H. Teow, W.L. Ang, Y.T. Chung, D.L. Oatley-Radcliffe, N. Hilal, Nanofiltration membranes review: recent advances and future prospects, *Desalination*, 356 (2015) 226–254.
- [23] A. Somrani, A.H. Hamzaoui, M. Pontie, Study on lithium separation from salt lake brines by nanofiltration (NF) and low pressure reverse osmosis (LPRO), *Desalination*, 317 (2013) 184–192.
- [24] W.R. Bowen, F. Jenner, Theoretical descriptions of membrane filtration of colloids and fine particles: an assessment and review, *Adv. Colloid Interface Sci.*, 56 (1995) 141–200.
- [25] J. Luo, L. Ding, Y. Su, S. Shao, Y. Wan, Concentration polarization in concentrated saline solution during desalination of iron dextran by nanofiltration, *J. Membr. Sci.*, 363 (2010) 170–179.
- [26] W.F. Blatt, A. Dravid, A.S. Michaels, L. Nelsen, Solute polarization and cake formation on membrane ultrafiltration: causes, consequences, and control techniques, J.E. Flinn, Ed., *Membrane Science and Technology*, Plenum Press, New York, 1970, pp. 47–97.
- [27] M.C. Porter, Concentration polarization with membrane ultrafiltration, *Ind. Eng. Chem. Prod. Res. Dev.*, 11 (1972) 234–248.
- [28] V. Gekas, B. Hallström, Mass transfer in the membrane concentration polarization layer under turbulent cross flow: I. Critical literature review and adaptation of existing sherwood correlations to membrane operations, *J. Membr. Sci.*, 30 (1987) 153–170.
- [29] G. Schock, A. Miquel, Mass transfer and pressure loss in spiral wound modules, *Desalination*, 64 (1987) 339–352.
- [30] E.R. Gilliland, T.K. Sherwood, Diffusion of vapors into air streams, *Ind. Eng. Chem.*, 26 (1934) 516–523.
- [31] A.R.D. Costa, A.G. Fane, C.J.D. Fell, A.F.M. Franken, Optimal channel spacer design for ultrafiltration, *J. Membr. Sci.*, 62 (1991) 275–291.
- [32] A.G. Volkov, S. Paula, D.W. Deamer, Two mechanisms of permeation of small neutral molecules and hydrated ions across phospholipid bilayers, *Bioelectrochem. Bioenerg.*, 42 (1997) 153–160.
- [33] G. Yang, H. Shi, W. Liu, W. Xing, N. Xu, Investigation of Mg^{2+}/Li^+ separation by nanofiltration, *Chin. J. Chem. Eng.*, 19 (2011) 586–591.
- [34] A.E. Childress, M. Elimelech, Relating nanofiltration membrane performance to membrane charge (electrokinetic) characteristics, *Environ. Sci. Technol.*, 34 (2000) 3710–3716.
- [35] M. Elimelech, W.H. Chen, J.J. Waypa, Measuring the zeta (electrokinetic) potential of reverse osmosis membranes by a streaming potential analyzer, *Desalination*, 95 (1994) 269–286.
- [36] A.E. Childress, M. Elimelech, Effect of solution chemistry on the surface charge of polymeric reverse osmosis and nanofiltration membranes, *J. Membr. Sci.*, 119 (1996) 253–268.
- [37] O. Kedem, A. Katchalsky, Permeability of composite membranes. Part 1. Electric current, volume flow and flow of solute through membranes, *Trans. Faraday Soc.*, 59 (1963) 1918–1930.
- [38] J. Straatsma, G. Bargeman, H.C.V.D. Horst, J.A. Wesselingh, Can nanofiltration be fully predicted by a model? *J. Membr. Sci.*, 198 (2002) 273–284.
- [39] G. Hagemeyer, R. Gimbel, Modelling the salt rejection of nanofiltration membranes for ternary ion mixtures and for single salts at different pH values, *Desalination*, 117 (1998) 247.
- [40] G. Bargeman, J.M. Vollenbroek, J. Straatsma, C.G.P.H. Schroën, R.M. Boom, Nanofiltration of multi-component feeds. Interactions between neutral and charged components and their effect on retention, *J. Membr. Sci.*, 247 (2005) 11–20.
- [41] W.R. Bowen, A.W. Mohammad, Characterization and prediction of nanofiltration membrane performance—a general assessment, *Chem. Eng. Res. Des.*, 76 (1998) 885–893.
- [42] P. Aimar, R. Field, Limiting flux in membrane separations: a model based on the viscosity dependency of the mass transfer coefficient, *Chem. Eng. Sci.*, 47 (1992) 579–586.
- [43] O.F.V. Meien, R. Nobrega, Ultrafiltration model for partial solute rejection in the limiting flux region, *J. Membr. Sci.*, 95 (1994) 277–287.
- [44] J. Luo, Y. Wan, Effects of pH and salt on nanofiltration—a critical review, *J. Membr. Sci.*, 438 (2013) 18–28.
- [45] R. Jiratananon, A. Sungpet, P. Luangsowan, Performance evaluation of nanofiltration membranes for treatment of effluents containing reactive dye and salt, *Desalination*, 130 (2000) 177–183.
- [46] A. Szymczyk, P. Fievet, Investigating transport properties of nanofiltration membranes by means of a steric, electric and dielectric exclusion model, *J. Membr. Sci.*, 252 (2005) 77–88.
- [47] A. Szymczyk, P. Fievet, Ion transport through nanofiltration membranes: the steric, electric and dielectric exclusion model, *Desalination*, 200 (2006) 122–124.
- [48] A.E. Yaroshchuk, Dielectric exclusion of ions from membranes, *Adv. Colloid Interface Sci.*, 85 (2000) 193–230.
- [49] X. Li, C. Zhang, S. Zhang, J. Li, B. He, Z. Cui, Preparation and characterization of positively charged polyamide composite nanofiltration hollow fiber membrane for lithium and magnesium separation, *Desalination*, 369 (2015) 26–36.
- [50] S. Bandini, D. Vezzani, Nanofiltration modeling: the role of dielectric exclusion in membrane characterization, *Chem. Eng. Sci.*, 58 (2003) 3303–3326.
- [51] L.A. Richards, M. Vuachère, A.I. Schäfer, Impact of pH on the removal of fluoride, nitrate and boron by nanofiltration/reverse osmosis, *Desalination*, 261 (2010) 331–337.
- [52] M. Mänttäri, A. Pihlajamäki, M. Nyström, Effect of pH on hydrophilicity and charge and their effect on the filtration efficiency of NF membranes at different pH, *J. Membr. Sci.*, 280 (2006) 311–320.
- [53] J.J. Qin, M.H. Oo, H. Lee, B. Coniglio, Effect of feed pH on permeate pH and ion rejection under acidic conditions in NF process, *J. Membr. Sci.*, 232 (2004) 153–159.
- [54] C. Mazzoni, L. Bruni, S. Bandini, Nanofiltration: role of the electrolyte and pH on Desal DK performances, *Ind. Eng. Chem. Res.*, 46 (2007) 2254–2262.